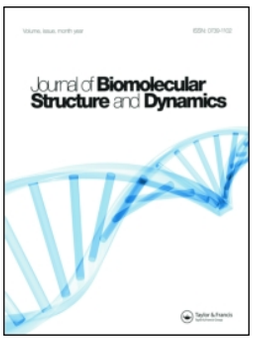

Journal of Biomolecular Structure and Dynamics

ISSN: 0739-1102 (Print) 1538-0254 (Online) Journal homepage: http://www.tandfonline.com/loi/tbsd20

An anti-DNA antibody prefers damaged dsDNA over native

N.I. Akberova, A.A. Zhmurov, T.A. Nevzorova & R.I. Litvinov

To cite this article: N.I. Akberova, A.A. Zhmurov, T.A. Nevzorova & R.I. Litvinov (2017) An anti-DNA antibody prefers damaged dsDNA over native, Journal of Biomolecular Structure and Dynamics, 35:1, 219-232, DOI: 10.1080/07391102.2015.1128979

To link to this article: http://dx.doi.org/10.1080/07391102.2015.1128979

Journal of Biomolecular Structure and Dynamics,
Vol. 35, No. 1, 219–232, http://dx.doi.org/10.1080/07391102.2015.1128979

Taylor & Francis
Taylor & Francis Group

An anti-DNA antibody prefers damaged dsDNA over native

N.I. Akberova[a], A.A. Zhmurov[b], T.A. Nevzorova[a] and R.I. Litvinov[c]*

[a]*Department of Biochemistry and Biotechnology, Institute of Fundamental Medicine and Biology, Kazan Federal University, 18 Kremlyovskaya St., Kazan 420111, Russian Federation;* [b]*Moscow Institute of Physics & Technology, 9 Institutskiy Per., Dolgoprudny, Moscow Region 141700, Russian Federation;* [c]*Department of Cell and Developmental Biology, University of Pennsylvania Perelman School of Medicine, 1109 BRB II/III, 421 Curie Blvd., Philadelphia, PA 19104-6058, USA*

Communicated by Ramaswamy H. Sarma

(*Received 11 August 2015; accepted 3 December 2015*)

DNA–protein interactions, including DNA–antibody complexes, have both fundamental and practical significance. In particular, antibodies against double-stranded DNA play an important role in the pathogenesis of autoimmune diseases. Elucidation of structural mechanisms of an antigen recognition and interaction of anti-DNA antibodies provides a basis for understanding the role of DNA-containing immune complexes in human pathologies and for new treatments. Here we used Molecular Dynamic simulations of bimolecular complexes of a segment of dsDNA with a monoclonal anti-DNA antibody's *Fab*-fragment to obtain detailed structural and physical characteristics of the dynamic intermolecular interactions. Using a computationally modified crystal structure of a *Fab*–DNA complex (PDB: 3VW3), we studied *in silico* equilibrium Molecular Dynamics of the *Fab*-fragment associated with two homologous dsDNA fragments, containing or not containing dimerized thymine, a product of DNA photodamage. The *Fab*-fragment interactions with the thymine dimer-containing DNA was thermodynamically more stable than with the native DNA. The amino acid residues constituting a paratope and the complementary nucleotide epitopes for both *Fab*–DNA constructs were identified. Stacking and electrostatic interactions were shown to play the main role in the antibody–dsDNA contacts, while hydrogen bonds were less significant. The aggregate of data show that the chemically modified dsDNA (containing a covalent thymine dimer) has a higher affinity toward the antibody and forms a stronger immune complex. These findings provide a mechanistic insight into formation and properties of the pathogenic anti-DNA antibodies in autoimmune diseases, such as systemic lupus erythematosus, associated with skin photosensibilization and DNA photodamage.

Keywords: anti-DNA antibody; dsDNA; immune complex; thymine dimer; Molecular Dynamics simulation

Introduction

Antibodies to native double-stranded DNA are present in the blood of healthy people, but their level is increased manifold in patients with autoimmune diseases, such as systemic lupus erythematosus (SLE) (Hahn, 1998; Yung & Chan, 2008). Antibodies to DNA play an important role in the pathogenesis of autoimmune lesions because immune DNA–antibody complexes can cause cell and tissue damages, although the mechanisms of their pathogenic action remains largely unknown. The vast majority of antibodies to DNA circulating in the blood of patients and healthy subjects are not associated with any pathologic manifestations and are non-pathogenic. Only a subset of antibodies to DNA circulating in the blood of patients are pathogenic because they are associated with one of the most common complications of SLE known as the "lupus" glomerulonephritis, a kidney damage followed by renal dysfunction (Greenspan et al., 2012; Krishnan, Wang, & Marion, 2012).

The differences in the structure and properties of pathogenic and non-pathogenic antibodies to DNA are not known. The molecular basis of antigenicity of different types of DNA, including chemically modified variants, is also unclear (Akagawa et al., 2006). Therefore, elucidation of the structural mechanisms of the polynucleotide antigen recognition and interactions of anti-DNA antibody with DNA provides insights into understanding the role of DNA-containing immune complexes in the pathogenesis of autoimmune diseases, and can form a foundation for new treatments that would specifically inhibit production of pathogenic antibodies and their interaction with DNA and other autoantigens. Furthermore, DNA–antibody complex can be considered as an analog of specific DNA–protein interactions, which may yield additional information about the intracellular regulatory mechanisms of transcription, mitosis, etc.

Although the structural basis of the interaction of anti-DNA antibodies is a fundamental problem of immunology, X-ray crystallographic studies of DNA–antibody complexes are exceptional (Herron et al., 1991; Mol, Muir, Cygler, Lee, & Anderson, 1994; Pokkuluri et al., 1994; Yokoyama et al., 1999, 2000). First of all,

*Corresponding author. Email: litvinov@mail.med.upenn.edu

this is due to difficulties in crystallization of the large molecular structures with flexible and unstructured portions. Despite the great value of X-ray crystallography, it describes a static molecular structure, while antibody–DNA interactions are highly dynamic. A protein as well as a polynucleotide can change their conformations and their functional groups may be displaced to enable them to contact each other. Unfortunately, the spatial resolution of experimental methods does not allow studying dynamics of proteins and nucleic acids at the atomic level. Therefore, the computer-based Molecular Dynamics (MD) simulation play an increasingly important role, as it "revives" crystallographic protein structures and provides information not available by other means about their moving parts and intra- and intermolecular interactions.

In this paper, the interactions of a 64M-5 antibody *Fab*-fragment with a double-stranded DNA segment were studied *in silico* by MD methods. The equilibrium structures containing or not containing thymine dimers in DNA were calculated. The amino acid residues constituting a paratope and the complementary nucleotide epitopes in the DNA molecules have been identified. It was found that in the contacts of the antibody with dsDNA stacking and electrostatic interactions play a major role, while hydrogen bonds are less important. Interactions of the *Fab*-fragment with the structural variants of DNA containing and not containing the thymine dimer were quantified using thermodynamic parameters.

Methods

Structural models of Fab–*DNA complexes*

The crystallographic structure of a 64M-5 *Fab*-antibody fragment bound to a double-stranded DNA fragment containing covalent thymine dimer (PDB ID: 3VW3) (Kobayashi et al., 1999) served as the basic initial model. The thymine dimer-containing DNA is a product formed upon UV-irradiation of DNA. The following amino acid residues that were not resolved by the X-ray crystallography were added to the *Fab*-fragment by means of the VMD program (Humphrey, Dalke, & Schulten, 1996): Asn135, Val193, Pro194, Ser195 – to the heavy chain, Asp1 and Glu213 – to the light chain. The numbering of amino acid residues of the *Fab*-fragment's light and heavy chains corresponds to the unified nomenclature for antibodies (Kabat, Wu, Perry, Gottesman, & Foeller, 1991).

Then, energy minimization for the modified structure was performed twice: for the first time, with the fixed amino acid residues whose coordinates were known from the crystal structure; for the second time, with the unfixed amino acid residues. Two similar constructs were prepared for computational experiments: ABDNA_TT (in which a covalent bond between T9 and T10 in the DNA's A-strand was retained from the original 3VW3 structure) and ABDNA (without the covalent T9-T10 bond in the DNA). Both constructs were placed in a water cell with $82 \times 75 \times 130$ Å dimensions and Na^+ and Cl^- ions were added at a concentration of 150 mM in order to keep a physiological ionic strength and pH 7.4. The final dissolved ABDNA_TT construct contained 78,235 atoms and ABDNA contained 78,231 atoms. We minimized the energy of the system for 100,000 steps using a combination of conjugate gradient and line search algorithms, which is a default option in NAMD (Phillips et al., 2005). Then, both constructs were subjected to heating up to 300 K with the subsequent energy equilibration.

Computing of the equilibrium MD of the Fab–*DNA complexes*

Computation and analysis were made in NAMD 2.10 CUDA multicore program (Phillips et al., 2005) with the use of the CHARMM 36 force field parameters (Foloppe & MacKerell, 2000; MacKerell et al., 1998). For the production run, we used a time step of 1 fs with no rigid bonds enabled. Throughout the simulation run, periodic boundary conditions were used. Long-range electrostatics was computed using a PME method with the PME cell size not exceeding 1 Å. For non-bonded interactions, a switching function was enabled with a switching distance of 8 Å and a cut-off distance of 12 Å. The list of pairs was updated every 10 steps with a 13.5-Å cut-off. To control the pressure, Berendsen barostat was enabled with a target pressure set to 1 atm. The relaxation time and compressibility were set to 1 ps and 4.57×10^{-5} bar^{-1} (Berendsen, Postma, van Gunsteren, DiNola, & Haak, 1984). Temperature coupling was enabled and set to a target temperature of 300 K. The durations of simulation runs were > 100 ns for both ABDNA_TT and ABDNA systems.

For quantitative analysis and visualization of MD simulations we used VMD 1.9 program (Phillips et al., 2005) and specially written scripts for comparing the constructs, determination of interatomic distances, RMSF and energy calculations, and mapping of contacts. The hydrophobic contacts were analyzed using a web service PLATINUM (Pyrkov, Chugunov, Krylov, Nolde, & Efremov, 2009), atomic coordinates at the last step of the MD simulations were used for the calculations.

Statistical analysis

Data processing and statistical analysis were performed using the *R* language in the RStudio software environment. For fitting analysis quantile–quantile (QQ) plots were built, the evaluation of distribution parameters in

fitting was carried out by the method of maximum likelihood estimation, testing the hypothesis of empirical and theoretical distributions agreement was performed using the Kolmogorov–Smirnov test (Ricci, 2005). To assess if the differences were significant when comparing averages of the interaction energies, contact areas, and values of the evaluation function between ABDNA_TT and ABDNA, the Student's *t*-test for equal variances was applied. Variance uniformity was determined by the Fischer's *F*-test (Krijnen, 2009).

To study protein motions, the principal component analysis (PCA) and the normal mode analysis (NMA) were performed on trajectories of the ABDNA_TT and ABDNA constructs using the Bio3D package in R (Grant, Rodrigues, ElSawy, McCammon, & Caves, 2006). Correlated atomic motions in ABDNA_TT and ABDNA were obtained by analyzing the dynamical cross-correlation map (DCCM) of C_α atoms using Bio3D.

Results

General structural characterization of the Fab*–DNA complexes*

Two related *Fab*–DNA constructs were studied and compared in this work, one containing a stretch of native DNA (ABDNA) and the other containing a homologous but chemically modified DNA fragment with a covalent intra-A-chain T9-T10 thymine dimer (ABDNA_TT). The 3D structures of ABDNA_TT and ABDNA obtained after 100 ns equilibrium simulations are shown in Figure 1. In both immune complexes, the DNA strands were partially separated and the loop of the *Fab*-fragment's light chain that represents the hypervariable region (V_L-CDR1) was inserted into the gap between the DNA strands. Removal of a covalent bond between the thymine bases (ABDNA) changed the orientation of the DNA fragment relative to the antigen-binding *Fv*-region without dissociation of the immune complex. Breaking the covalent bond in the thymine dimer induced a moderate rearrangement of the overall *Fab*–DNA structure, namely a shift of amino acid residues and changes of interatomic distances in the contact regions. Superposition of the ABDNA_TT and ABDNA constructs (Figure 1(a)) revealed their conformational differences. The most flexible structures of the *Fab*–DNA complexes were the polynucleotide strands. In general, breakage of the covalent bond in the DNA thymine dimer enlarged the gap (or the interatomic distances) between the *Fab* amino acid residues and DNA nucleotides, indicating weakening of the complex formed by the *Fab*-antibody and the antigen.

Some representative changes in the relative positions of the atoms involved in the interactions between *Fab* and DNA in the presence (ABDNA_TT) and absence (ABDNA) of the T-T dimer are shown in Figures 1(b)–(d) and S1 (Supplementary Material). E.g. after breaking covalent bond in the thymine dimer the side groups of the *Fab*'s light chain residues Tyr32 (Figure 1(b)) and His27d (Supplementary Figure S1(a)) moved away from the phosphate groups of thymines T9 and T10 in the DNA's A-chain. An increase in interatomic distances in the vast majority of contacts between *Fab* and DNA after breakage of the T-T bond was observed throughout the entire trajectories of the equilibrium MD simulations. E.g. the distances between the ε-hydrogen of the *Fab*'s light chain residue His27d and oxygen atoms of the phosphate group in the DNA A-chain's thymine 10 in ABDNA construct (Supplementary Figure S1(b), dashed line) during 40 ns simulation were larger than the distances between these same atoms in the ABDNA_TT construct containing the T-T dimer (Supplementary Figure S1(b), solid line).

Rupture of the T-T crosslink also resulted in that the *Fab*'s light chain peptide backbone moved away from DNA as evidenced, for example, by an increase in the distance between a phosphate atom of the phosphate group of adenine 8 in the DNA's B-chain and a hydrogen atom of the amino group in the *Fab*'s light chain residue Gln27 (Figure 1(c)). Another example is an increase in the distance between an oxygen atom of the phosphate group of thymine 10 in the DNA's A-chain and a nitrogen atom of the amino group in the *Fab*'s light chain residue His93 in the ABDNA construct without a T-T dimer (Supplementary Figure S1(c)).

At the same time, quite rarely, atoms that belong to *Fab* and DNA got closer due to a turn of the amino acid residues and nitrogenous bases in response to rupture of the T-T bond; however, such shift toward tighter contacts in ABDNA vs. ABDNA_TT was not typical.

The observed conformational differences between ABDNA_TT and ABDNA were likely due to DNA bending caused by the T-T dimer (best seen in Figure 1(a)), which partially straightened after removal of the thymine dimer from the A-chain of DNA.

Flexible portions of the Fab*-fragment and DNA*

Analysis of atomic fluctuations during MD simulations enabled us to reveal the most mobile groups of atoms and to identify areas in *Fab* and DNA which undergo structural rearrangements in response to formation or breakage of the thymine dimer. We calculated the root mean square fluctuation (RMSF), which is an average deviation of atoms relative to a reference position, as a measure of flexibility of polypeptide or polynucleotide chains. Figure 2 shows the values of RMSF for DNA nucleotides in the A- and B-strands and for amino acid residues of the heavy and light chains of the *Fab*-fragment. As shown in

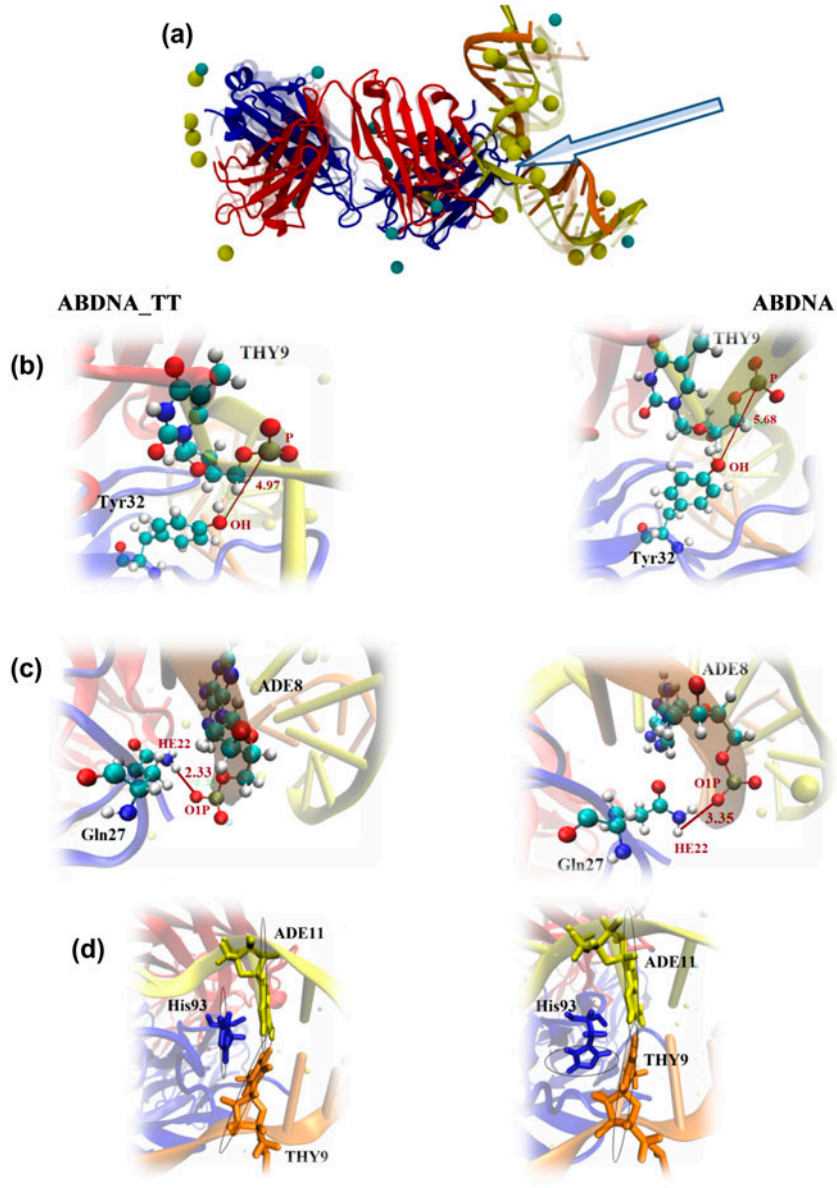

Figure 1. Structure of ABDNA_TT and ABDNA after 100-ns simulation: the *Fab*-fragment's H-chain is shown in red, the L-chain in blue: the A and B strands of DNA are shown in yellow and orange, respectively. (a) Superposition of the constructs with and without the thymine dimer: ABDNA is shown with bright colors, ABDNA_TT – with pale, transparent colors. Arrow shows the light chain loop (V_L-CDR1) between the strands of DNA. The figure shows Na^+ (yellow balls) and Cl^- (cyan balls). (b) Examples of electrostatic interactions and (c) hydrogen bonds formed between *Fab* and DNA. The nucleotides and amino acid residues in the contacts are represented using balls and sticks and colored by chemical elements. The distances between atoms are shown in purple. (d) Complex stacking interactions between His93 in the *Fab*'s light chain, adenine 11 of the DNA's A-strand, and thymine 9 of the DNA's B-strand. The nucleotides and amino acid residues in the contacts are represented using sticks in accordance with the color of the chain to which they belong. The aromatic rings planes are marked by ellipses.

Figure 2(a), the central portion of the A-strand in the T-T dimer-containing ABDNA_TT and the corresponding area in the T-T dimer-free ABDNA were almost immobile, while the end portions of the DNA fragment showed substantially larger fluctuations in both constructs. In the native DNA, there were some peaks in fluctuations of adenine at position 10 and especially of thymine at position 12 in the DNA's B-chain in both *Fab*–DNA constructs. It is noteworthy that breaking covalent bond in the thymine dimer (ABDNA) led to an increase in the flexibility of the T12-G13-A14-A15 region in the A-strand of DNA. After breaking the T-T bond in the A-strand the nitrogenous bases in the B-strand of DNA became more mobile within positions 2–9. The observed RMSF increase in ABDNA

compared to ABDNA_TT indicates that rupture of the T-T dimer results in a partial impairment of the interactions between the 64M-5 antibody *Fab*-fragment and DNA.

In both the ABDNA and ABDNA_TT constructs, substantially more contacts with DNA were found to be located in the light chain than in the heavy chain of *Fab* (Tables 1 and 2). This observation suggests that breakage or formation of the thymine dimer must result in more pronounced changes of the mobility of amino acid residues located in the *Fab*'s light chain. However, as shown in Figure 2(b), the RMSF profiles for the *Fab*-fragment's light chain were almost identical in the presence and absence of the thymine dimer in DNA. The flexibility of amino acid residues in the *Fab*-fragment's heavy chain (Figure 2(c)) was also similar in ABDNA and ABDNA_TT, but without the thymine dimer (ABDNA) the mobility of some amino acid residues was reduced (Figure 2(c)). The dependence of RMSF on the positions of amino acid residues in the *Fab*-fragment's heavy and light chains indicated that their mobility was variable, and the largest fluctuations were typical for the *C*-termini of the polypeptide chains. In the light chain, the lowest mobility was detected in the areas interacting with the heavy chain (positions 40–42, 52) and for the residues forming the CDR2-loop (positions 70–75). In the heavy chain, a lower mobility was characteristic for the residues directly interacting with DNA. RMSF analysis of the heavy and light chains in ABDNA and ABDNA_TT showed that there were no significant changes in the interface between the heavy and light chains upon removal of the thymine dimer from DNA.

In order to identify major components of the molecular motion during the equilibrium simulations, the PCA was performed on trajectories for the ABDNA_TT and ABDNA structures. The first Principal Component (PC1) for both systems was identified as bending of the entire molecule around the hinge in the central part of *Fab* (Supplementary Figure S7(a) and (b)). The second Principal Component (PC2) was different for ABDNA and ABDNA_TT, although in both systems PC2 was related to the motions of amino acid residues adjacent to the *Fab*–DNA-binding interface. In ABDNA, PC2 was

Table 1. Contacts between the *Fab*-fragment and DNA common to ABDNA_TT and ABDNA.

						ABDNA_T-T		ABDNA	
DNA strand	Nucleotide	Nucleotide position	*Fab* chain[a]	Amino acid residue	Amino acid number	Occupancy, %	[b]Interaction type	Occupancy, %	[b]Interaction type
A	**A**	11	L	**H**	93	100	S	42.1	S
A	**T**	10	L	**S**	92	98.1	E	100	E
A	**T**	10	L	**H**	27d	100	E	100	E
A	**T**	9	L	**N**	28a	99.9	E	100	E
A	**A**	8	L	**N**	28a	66.3	E	90.3	E
A	**T**	10	L	**N**	28	73.8	E	60.4	E
A	**A**	8	L	**N**	28a	66.3	E	90.4	HB
A	**T**	10	L	**H**	93	100	E	71.6	HB
A	**T**	10	L	**H**	93	91.7	HB	71.6	HB
A	**T**	10	H	**W**	33	100	S	100	S
A	**T**	9	H	**Y**	100i	92.3	S	88.8	S
A	**T**	9	H	**Y**	97	58.2	S	81.4	S
A	**A**	11	H	**T**	58	100	E	100	E
A	**A**	11	H	**T**	58	58.2	HB	100	E
A	**T**	9	H	**R**	95	83.7	HB	90.9	HB
A	**A**	11	H	**T**	58	100	E	88.6	HB
A	**A**	11	H	**T**	58	58.2	HB	88.6	HB
B	**T**	9	L	**H**	93	100	S	98.2	S
B	**A**	11	L	**Y**	30	70.5	S	46.5	S
B	**A**	10	L	**S**	27e	99.9	E	100	E
B	**A**	8	L	**Q**	27	100	E	95.7	E
B	**A**	8	L	**Q**	27	70.2	HB	95.7	E
B	**T**	9	L	**N**	27a	99.6	E	77.9	E
B	**T**	9	L	**N**	27a	93.1	HB	77.9	E
B	**A**	10	L	**N**	27a	99.4	E	76.1	E
B	**C**	7	L	**Q**	27	73.4	E	68.6	E
B	**T**	9	L	**Q**	27	95.5	E	66.5	E
B	**A**	8	L	**Q**	27	100	E	62.4	HB
B	**A**	8	L	**Q**	27	70.2	HB	62.4	HB

[a]*Fab* chains: H – heavy, L – light.
[b]Interaction types: S – stacking, E – electrostatic, HB – hydrogen bonds.

Table 2. Contacts between the *Fab*-fragment and DNA unique to ABDNA_TT or ABDNA.

DNA strand	Nucleotide	Nucleotide position	*Fab* chain[a]	Amino acid residue	Amino acid number	ABDNA_TT		ABDNA	
						Occupancy, %	[b]Interaction type	Occupancy, %	[b]Interaction type
A	**A**	8	L	**Y**	30	99.3	S	–	–
A	**A**	8	L	**Y**	32	65.8	S	–	–
A	**T**	9	L	**Y**	32	42.6	S	–	–
A	**T**	9	L	**H**	27d	99.8	E	–	–
A	**T**	10	L	**N**	28	58.0	E	–	–
A	**A**	8	L	**Y**	32	55.3	HB	–	–
A	**A**	8	H	**Y**	100i	96.9	S	–	–
A	**T**	10	H	**H**	35	61.6	S	–	–
A	**T**	9	H	**W**	33	59.3	S	–	–
A	**T**	9	H	**N**	96	96.0	HB	–	–
B	**A**	8	L	**S**	26	93.4	E	–	–
B	**C**	6	H	**Q**	61	52.8	E	–	–
A	**A**	11	L	**H**	27d	–	–	60.9	S
A	**T**	9	L	**N**	28	–	–	99.2	E
B	**T**	9	L	**H**	27d	–	–	74.6	S
B	**A**	11	L	**S**	27e	–	–	100	E

[a]*Fab* chains: H – heavy, L – light.
[b]Interaction types: S – stacking, E – electrostatic, HB – hydrogen bonds.

overall more pronounced, especially for the residues in the light chain's loop Ser26-Thr31, which was the closest loop to the T-T dimer (loop 1 on Supplementary Figure S7). In ABDNA_TT, the motion along PC2 was more subtle and involved mostly the heavy chain (loops 3 and 4 on Supplementary Figure S7).

Results of the NMA performed for ABDNA and ABDNA_TT MD-trajectories revealed almost identical spectra of normal eigenfrequencies and scales of normal displacements of the light and heavy chains from the global modes for ABDNA and ABDNA_TT (Supplementary Figure S8(e)). The normal modes themselves resembled rotational and oscillator motions of the *Fab*-fragment around the central "hinge" (Supplementary Figure S8(a)–(c)) as well as a motion of the entire binding cluster away from the DNA (Supplementary Figure S8(d)). The dynamical cross-correlation maps of Cα atoms also showed distinctions in the correlated atomic motion in the ABDNA_TT and ABDNA constructs, including the sites of interaction with DNA.

Binding interface between the Fab-*fragment and DNA*

A step-by-step analysis of the MD coordinate files allowed identification of individual atoms and groups of atoms that were directly involved in the interactions of the *Fab*-fragment with DNA. We defined the contacts as follows. If charged groups of two residues of an amino acid and a nucleotide were within 8 Å, these residues were considered as forming an electrostatic contact. A stacking contact was recorded when the centers of mass of two aromatic rings were within 7 Å. Two residues were considered as forming a hydrogen bond if the distance between the hydrogen atom and its acceptor was within 4 Å and the bond angle was less than 40° from the straight line. Table 1 shows 29 contacts between the DNA bases and amino acid residues of the *Fab*-fragment that were common to both constructs (ABDNA_TT and ABDNA) and that were detected at all steps of MD in all trajectories. These contacts were characterized by a high incidence within the *Fab*–DNA interface shown as the occupancy numbers in Tables 1 and 2. To compute the occupancy, we first found which contacts were existent for each coordinate snapshot (a frame). The occupancy of each contact was then calculated as a ratio of the number of frames where this contact existed over the total number of frames. Only contacts with the occupancy larger than 50% are shown. In addition, some contacts were identified that were unique for each of the studied constructs, ABDNA_TT and ABDNA. Twelve interatomic contacts formed exclusively in the *Fab*–DNA construct containing the thymine dimer and four contacts were unique for the construct without the T-T dimer (Table 2). A smaller number of the unique contacts in ABDNA suggest that breaking of the T-T bond in the DNA's A-strand results in a lower affinity of *Fab* to DNA. Contact maps (Supplementary Figures S3 and S4), which display the interaction spots of the *Fab*-fragment's light and heavy chains with the DNA strands, were based on a detailed structural analysis. The heavy chain of the *Fab*-fragment interacted mainly with the DNA's A-strand and the total number of DNA contacts with the *Fab*'s heavy chain (13) was less than the number of DNA contacts with the light chain (32). The following

regions of the *Fab*-fragment formed the largest part of the *Fab*–DNA interface: Ser26-Tyr32, Gly91, and Thr97 in the light chain and Trp33, His35, Thr58, Lys62, and Arg95-Tyr100i in the heavy chain.

Physical nature of the bonds between Fab *and DNA*

The contacts between the *Fab*-fragment's CDRs and the DNA antigen most often were mediated by electrostatic interactions (49%), stacking interactions (31%), and hydrogen bonds (~20%) (Table 1). It is noteworthy that the unique (most specific) contacts of the *Fab*-fragment with ABDNA_TT or ABDNA (Table 2), unlike the common bonds (Table 1), were represented mainly by the stacking (50%) and electrostatic (~38%) interactions. It was found that breaking the thymine dimer modified the type of interactions between some residues of the *Fab*-fragment and DNA nucleotides. E.g. the *Fab*'s light chain residue Tyr32 interacted with T9 of the thymine dimer in the DNA's A-strand via a stacking interaction, while in the construct without the thymine dimer a weak hydrogen bond was found in this binding spot (Supplementary Figure S3). The same *Fab*'s light chain Tyr32 residue was involved in the stacking interaction with adenine A8 of the DNA's A-strand in ABDNA_TT, whereas in ABDNA there was no interaction between the same residue and nucleotide. The stacking interaction between Tyr30 in the *Fab*'s light chain and adenine A8 of DNA's A-chain was observed in ABDNA_TT, which vanished in ABDNA. Here are three other changes in the nature the interaction between *Fab* residues and DNA nucleotides after breaking the thymine dimer: the *Fab*'s light chain residues Asn28 and Ser98 interacted with T9 of the thymine dimer in the DNA's A-strand and the *Fab*'s light chain His93 interacted with T10 of the thymine dimer in the DNA's A-strand. In the last three pairs, a switch was observed from electrostatic interactions in ABDNA_TT to weaker hydrogen bonds in ABDNA. Figure 1(d) illustrates the positions of the *Fab*'s light chain residue His93, adenine A11 in the DNA's A-strand, and thymine T9 in the DNA's B-strand involved in the stacking interactions in ABDNA_TT and ABDNA. It is clearly seen that breaking the thymine dimer changed the type of interaction from the parallel stacking to the *T*-stacking structures. In addition, the occupancy of a stacking interaction between His93 and adenine A11 after breaking the thymine dimer dropped from 100% in ABDNA_TT down to 42% in ABDNA (Table 1). The light chain residue Tyr32 formed a typical *T*-stack with adenine A8 of DNA's A-strand and closer to the *T*-stacking structure with T9 of the thymine dimer in the DNA's A-strand in ABDNA_TT. After breaking the thymine dimer, the *T*-stacking interaction between the light chain Tyr32 and thymine T9 changed to the parallel stacking with a rare occupancy in ABDNA (Supplementary Figure S2(a)).

Significantly fewer contacts of DNA with the *Fab*'s heavy chain were found than with the light chain (Supplementary Figure S4); however, these interactions were also weaker in ABDNA compared to ABDNA_TT. Namely, the electrostatic interactions between the *Fab*'s heavy chain and the B-strand of DNA seen in ABDNA_TT were almost completely gone in ABDNA. Of six stacking pairs observed between the *Fab*'s heavy chain and the A-strand of DNA in ABDNA_TT only five remained in ABDNA, while the stacking interaction Trp33–T was substantially weakened, although not fully disappeared after breakage of the T-T dimer. We observed that in ABDNA_TT the heavy chain Trp33 formed a *T*-stack with thymine T9 and simultaneously a parallel stack with T10 of the thymine dimer in DNA's A-strand, while the latter turned into *T*-stack after breaking of covalent bond in the thymine dimer in ABDNA (Supplementary Figure S2(b)). Interestingly, two additional pairs of weak stacking interactions His35-T9 and Tyr97-A8 were identified in ABDNA. This is probably due to the fact that the π-π hydrophobic interactions of aromatic rings in nucleotides and amino acid residues are potentially labile with possible transitions between the face-to-face, edge-to-face, and parallel displaced stacking conformations (well seen in Supplementary Figure S2). Such resistance of stacking interactions to the structural changes suggests that they are largely responsible for stabilization of the immune antibody–DNA complex.

Thermodynamics of the interactions between the Fab*-fragment and DNA*

Using the NAMD program, we evaluated the total energy of non-covalent interactions between the *Fab* and DNA as well as the partial electrostatic and Van der Waals energies of these interactions at each step of MD. We then plot the distributions of these energies over the simulation runs for both ABDNA and ABDNA_TT systems (Figure 3). Fitting analysis of the electrostatic and the Van der Waals interactions energy histograms confirmed their normal distributions. The results show that thermodynamic stability of the *Fab*–DNA complex strongly depends on the presence of covalent crosslinking between the thymine bases as evidenced by the energy distributions of the electrostatic (Figure 3(a)) and Van der Waals (Figure 3(b)) interactions. The energy of the integral electrostatic interactions was -244 ± 33 kcal/mol for ABDNA_TT and -207 ± 31 kcal/mol for ABDNA (mean ± SD, $p < .001$). Analysis of the Van der Waals interactions in the *Fab*–DNA complex also indicated weakening of this type of interactions after the thymine dimer was removed from DNA. The total value for

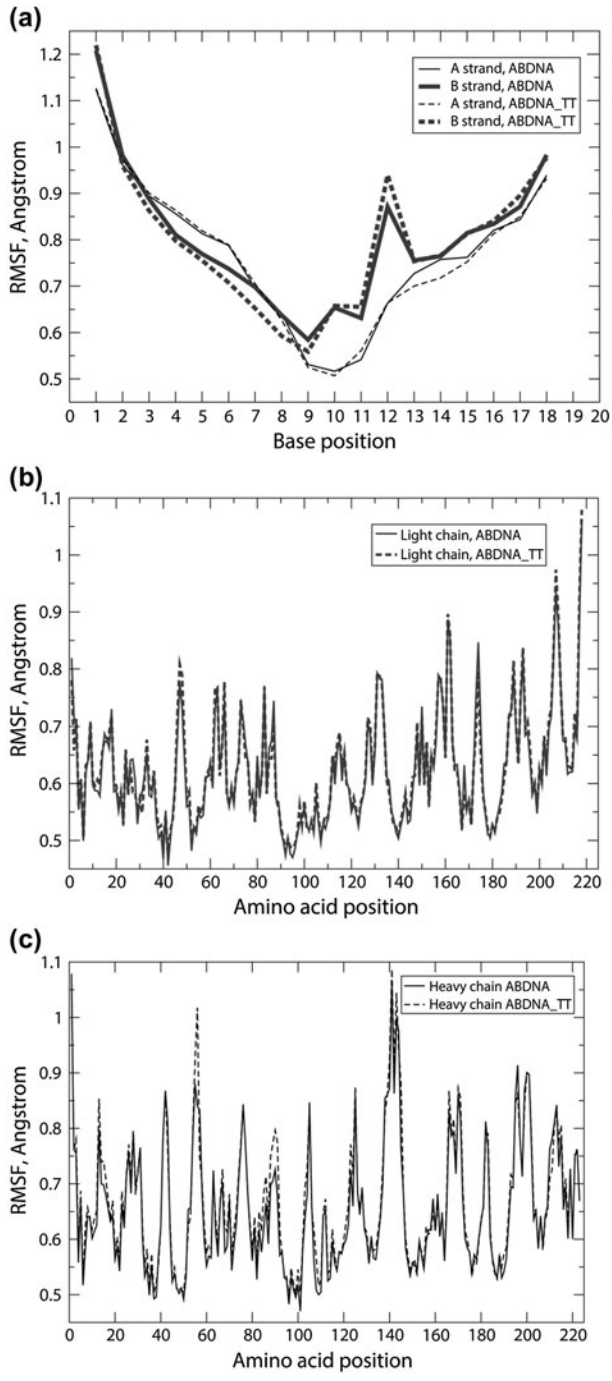

Figure 2. RMSF of nucleotides (a) and of amino acid residues of the light (b) and the heavy (c) chains of the *Fab*-fragment within the *Fab*–DNA constructs containing (ABDNA_TT) and not containing (ABDNA) the thymine dimer.

the average Van der Waals interactions was -122 ± 7 kcal/mol for ABDNA_TT vs. −108 ± 7 kcal/mol for ABDNA ($p < .001$). Quantification of stacking interactions also provided evidence for their significant weakening in ABDNA compared to ABDNA_TT. An integral unitless parameter characterizing a relative strength of stacking interactions or the so-called "estimator function" (Pyrkov et al., 2009), was smaller for ABDNA than for ABDNA_TT (1.83 ± .58 vs. 5.36 ± .72, respectively; $p < .05$). Taken together, these results show that the *Fab*–DNA construct with the thymine dimer is thermodynamically more stable and that breakage of the T-T bond leads to partial destabilization of the *Fab*–DNA complex.

Despite the overall weakening of *Fab*–DNA interactions after breaking the bond in the thymine dimer, in some quite few contacts the local interactions strengthened due to formation of new stacking or electrostatic interactions. E.g. a hydrogen bond between the *Fab*'s light chain His27d and A11 in the A-strand of DNA in ABDNA_TT was replaced with the stronger stacking interaction; the weak electrostatic interaction between the *Fab*'s light chain His27d and T9 in the B-strand of DNA in ABDNA_TT was replaced with the stacking interaction in ABDNA; a hydrogen bond between the *Fab*'s light chain His27d and A10 of the B-strand of DNA in ABDNA_TT changed to the electrostatic interactions after breaking the thymine dimer. However, the strengthening of contacts between *Fab* and DNA during the structural transition from ABDNA_TT to ABDNA was much less common than their weakening (Supplementary Figures S3, S4).

Discussion

Immune complexes of antibodies with DNA are exceptionally important objects with very special structure and properties. From the standpoint of structural biology, they represent protein–DNA complexes that are of fundamental importance for cell physiology. At the same time, the interactions of DNA with antinuclear antibodies are important players in the pathogenesis of autoimmune diseases, such as SLE and rheumatoid arthritis. Despite the presence of anti-DNA antibodies in the blood of patients in a much higher titer than in healthy subjects, there is only a subset of these antibodies associated with a disease state, hence referred to as "pathogenic" vs. "non-pathogenic" antibodies. Conditions of the formation of the pathogenic antibodies to DNA are not fully understood and may be related to the extracellular DNA appearing as a result of cellular damage due to apoptosis, necrosis, or autophagy (Dixit & Ali, 2001; Frese & Diamond, 2011; McHugh, 2002; Pisetsky, 2013; Rahman et al., 2002; Stuart & Hughes, 2002; Su & Pisetsky, 2009). It is likely that DNA undergoes chemical or some other structural modifications, thereby acquiring antigenic properties. An insight into the structural basis of molecular recognition and interactions with an antigen is crucial for understanding the pathogenic role of anti-DNA antibodies. Because the differences between pathogenic and

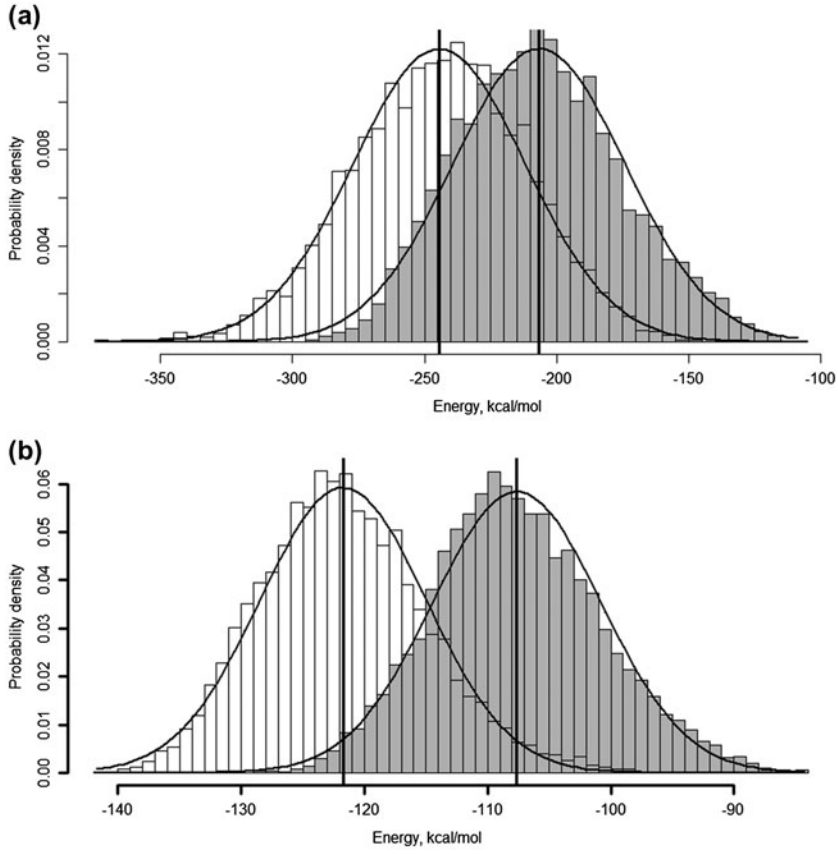

Figure 3. Energy distributions of the electrostatic interactions (a) and van der Waals interactions (b) between the *Fab*-fragment and DNA for ABDNA_TT (white bars) and ABDNA (gray bars).
Notes: The distributions are obtained over the 100 ns simulation runs (energy values were recorded during MD simulations every 10 ps). The histograms are fitted with a Gaussian function and the peak values are shown by vertical lines.

non-pathogenic antibodies to DNA perhaps are very small, a detailed structural analysis and MD are extremely important for understanding the mechanisms of antibody–DNA interactions.

In this work, the interaction of a 64M-5 anti-DNA antibody with DNA was studied using MD simulations of the crystallographically resolved complex of the antibody's *Fab*-fragment with a segment of DNA (PDB ID: 3VW3, Yokoyama, Mizutani, & Satow, 2013). By modifying computationally the original crystal structure of the *Fab*–DNA complex, we have built virtual constructs with the same *Fab*-fragment associated with two different but homologous segments of dsDNA. One of the DNA segments contained a covalent thymine dimer as a model of chemically modified polynucleotide antigen (photo adduct). The other DNA fragment contained no thymine dimer and represented a natural unmodified antigen (native dsDNA). The *Fab*-fragment studied comprised all six complementarity determining regions (CDRs) of the hypervariable regions of the light and heavy chains of antibodies and thus possessed the antigen-binding properties of the whole antibody molecule.

We showed that the amino acid residues of all six V_L and V_H CDRs were involved in the interactions with DNA and that a large loop V_L-CDR1 was located within a gap between the DNA strands, containing or not containing the thymine dimer (Figure 1). It is consistent with an earlier finding that V_L-CDR1 is involved in the recognition of DNA and possibly causes dissociation of its complementary strands (Hideshi & Ryuta, 2014; Radic & Weigert, 1994; Yokoyama & Mizutani, 2014). This interaction resembles a DNA repair protein UvrB, which has a β-loop inserted between the DNA strands to induce their separation (Truglio et al., 2006). It is well known that the structure of the β-loop is conserved among known UvrB proteins (Skorvaga, Theis, Mandavilli, Kisker, & Van Houten, 2002) and that the β-loop is essential for the recognition of damaged (e.g. photochemically modified) DNA (Moolenaar, Hoglund, & Goosen, 2001). Our results in combination with the literature strongly suggest that chemically modified or damaged DNA is a preferable ligand for anti-DNA antibodies and perhaps can induce their formation.

An important role that anti-DNA antibodies play in the pathogenesis of autoimmune diseases, including SLE, is related to the properties of modified or abnormal DNA formed in these pathological conditions. Patients with SLE are characterized by photosensitivity (increased sensitivity of the skin and mucosa to the light and UV radiation), which may lead to UV-induced DNA damage, causing the exposure of polynucleotide autoantigens (Casciola-Rosen, Wigley, & Rosen, 1997; Rosen & Casciola-Rosen, 2009). It is important that native mammalian DNA does not cause production of antibodies to DNA, while modifications or conformational changes of the molecule caused by radiation energy, active forms of oxygen, epigenetic changes may contribute to its immunogenicity (Ames, Alves, Murat, Isenberg, & Nourooz-Zadeh, 1999; Bach, Koutouzov, & Endert, 1998; Evans, Cooke, Akil, Samanta, & Lunec, 2000; Lunec et al., 1994; Maeshima, Liang, Otani, Mune, & Yukawa, 2002; Suwannaroj, Lagoo, Keisler, & McMurray, 2001; Utz, Hottelet, Schur, & Anderson, 1997; Waris & Alam, 2004; Waszczykowska et al., 1999; Waters et al., 2004). For that reason we have compared the amino acid sequences of the light and the heavy chains from the *Fab*-fragment of the antibody 64M-5 studied here, which is specific for dsDNA containing photoproducts, with the heavy and the light chains sequences of various antibodies shown to be involved in the pathogenesis of SLE (Supplementary Figure S6). A high degree of homology and a large number of conserved aromatics amino acid residues for both light and heavy chains were identified. This indicates a basic structural similarity of anti-DNA antibodies formed in SLE.

Obviously, a pathogenic potential of antibodies to DNA is associated with specificity and affinity to the antigen that are determined by the mosaic of certain amino acid residues in the hypervariable regions (CDR) of the H- and L-chains (Collis, Brouwer & Martin, 2003; Demaison, Chastagner, Theze, & Zouali, 1994; Dörner, Kaschner, Hansen, Pruss, & Lipsky, 2001; Foster, Kieber-Emmons, Ohliger, & Madaio, 1994; Fraser, Rowley, Field, & Stott, 2003; Suzuki, Harada, Mihara, & Sakane, 1996). Therefore, we compared the structure and mobility of the interfaces as well as the number, physical nature, and strength of the contacts formed by the *Fab*-fragment with a fragment of native or chemically modified DNA, i.e. not containing and containing the thymine dimer, respectively. Breakage of a covalent bond in the thymine dimer is followed by changes in the *Fab*'s conformation, orientation of amino acid residues, and in the interatomic distances within the contact spots, which altogether indicate weakening of the *Fab*–DNA complex (Supplementary Figures S3, S4). This is consistent with the earlier finding that the antibody 64M-5 is highly specific to the photo adducts in the double-stranded DNA (Morioka et al., 1998; Scrima et al., 2008). Comparison of energies of the electrostatic (Figure 3(a)) and van der Waals (Figure 3(b)) interactions in the ABDNA vs. ABDNA_TT directly indicates weakening of contacts between *Fab* and DNA, meaning that without thymine dimers in DNA the immune complex is thermodynamically less stable. Presumably, it is due to the fact that the removal of T-T dimers changes the geometry of DNA, making its interaction with the *Fab*-fragment thermodynamically less favorable.

The results of this study shed light on some common structural mechanisms of interaction of antibodies with DNA. According to our data, the light chain CDRs of the *Fab*-fragment form more contacts with DNA than the heavy chain (Supplementary Figure S3) and they interact with both DNA strands, whereas the residues of the *Fab*'s heavy chain CDRs touch only the A-strand of DNA (Supplementary Figure S4), although the heavy chain CDRs is thought to play a major role in antigen binding (Kuroda, Shirai, Jacobson, & Nakamura, 2012). Indeed, in many anti-DNA antibodies the ability to interact with DNA is inherent in the heavy chain, mainly due to the V_H-CDR3, and the light chain may only modulate this interaction (Behrendt, Partridge, Griffiths, & Goodfield, 2003; Bespalov, Bond, Purmal, Wallace, & Melamede, 1999; Cerutti, Centeno, Goldbaum, & de Prat-Gay, 2001; Hahn, 1998; Jang & Stollar, 2003; Radic & Seal, 1997; Vargas-Madrazo, Lara-Ochoa, & Carlos Almagro, 1995). Our results suggest that for the interaction with a damaged or modified DNA, unlike native DNA, the CDRs of both light and heavy chains are important (Kozyr et al., 2012). The following mechanism seems plausible: V_L-CDR1 plays a primary role in recognition of the damaged site [which is confirmed by the structural similarity of the antibody 64M-5 with DNA repairing enzymes (Yokoyama et al., 2013)], while the heavy chain CDRs are involved in the "correct" final orientation of the *Fab*-fragment and in stabilization of the *Fab*–DNA complex mainly due to formation of stacking contacts with DNA. Indeed, despite a fewer number of contacts of the *Fab*-fragment's heavy chain, we found that among them the stacking interactions prevail that are strong enough to prevent the *Fab*–DNA complex from dissociation upon removal of the thymine dimer.

Our results emphasize the importance of aromatic amino acid residues for the *Fab*–DNA interactions. In particular, we found that the aromatic amino acid residues Trp33, His35, Tyr 97, and Tyr100i participate in the interactions with DNA that are known to be important for the interaction of various antibodies with different antigens (Akiba & Tsumoto, 2015; Avnir et al., 2014; Hahn, 1998; Isenberg, Tucker, & Cambridge, 1997; Schuermann et al., 2004; Zein et al., 2011). To corroborate this conclusion, we performed alignment of multiple sequences homologous to the light and the heavy

chains of the antibody 64M-5 (Supplementary Figure S5); this analysis revealed that many aromatic amino acid residues in the CDRs of both light and heavy chains were present in various antigen-binding fragments. The comparative shares of aromatic structures in the total amino acid composition of the light and heavy chains of *Fab*-fragments and in their conserved regions are shown in Supplementary Table S1. Aromatics amino acids are engaged in the stacking interactions with the DNA bases and thus can orient the antibody relative to the antigen and stabilize the immune complex. In the T-T dimer area in ABDNA_TT, the residues of *Fab*'s both light and heavy chains form stacking interactions with both DNA strands. In the absence of the T-T bond in ABDNA, the physical nature of the *Fab* interactions with DNA is changed to induce their weakening. Therefore, we can assume that the variable regions of the *Fab*'s heavy chain are primarily responsible for the stability of the immune complex, while the light chain plays a major role in the recognition of damaged DNA by the antibody. Contact maps (Supplementary Figures S3 and S4) demonstrate that the interactions can be ranged by their importance for stability of the *Fab*–DNA complexes in the following order: stacking contacts, electrostatic interactions, and hydrogen bonds, which is largely consistent with the literature (Saul & Alzari, 1996; Sundberg, 2009).

Thus, the aggregate of data shows that the highly specific recognition and stability of DNA-containing immune complexes are governed primarily by the amino acid composition of both light and heavy polypeptide chains, by the number and location of the aromatic amino acid residues, and the geometry of the antigen. The anti-DNA antibody 64M-5 studied here preferably interacts with a modified DNA containing the thymine dimer compared to the native DNA.

Conclusions

Covalent dimerization of thymines 9 and 10 within the DNA's A-strand changes the antibody-binding properties of the DNA and induces conformational changes in the *Fab*–DNA immune complex followed by redistribution of the binding interface that leads to strengthening of the bonds between the *Fab*-fragment and the double-stranded DNA. This strengthening results from an increased number of direct *Fab*–DNA contacts, decreased flexibility of the interacting DNA and *Fab* portions, switches in the physical nature of *Fab*–DNA bonds toward stronger interactions, and an increase in the overall and partial binding energy. Collectively, these factors make the interaction of the anti-DNA antibody's *Fab*-fragment with a chemically modified (photo damaged) DNA more favorable than with a native dsDNA.

The interaction of a monoclonal antibody with a double-stranded DNA is mediated by the amino acid residues of V_L and V_H CDRs and the light chain's CDR1 is inserted into the gap between the DNA strands. The most frequent bonds between the CDRs and DNA are electrostatic interactions (49%), stacking interactions (31%) and hydrogen bonds (20%). The contacts that determine the binding specificity of the antibody and DNA (i.e. observed in the *Fab*–DNA complex with thymine dimer but not observed in the complex without dimer) are almost entirely represented by the stacking (50%) and electrostatic (~38%) interactions.

Abbreviations

ABDNA	complex of the antibody's *Fab*-fragment with a DNA segment not containing thymine dimers
ABDNA_TT	a complex of the antibody's *Fab*-fragment with a DNA segment containing thymine dimers
T-T	thymine dimer
SLE	systemic lupus erythematosus
PDB	Protein Data Bank
VMD	Visual Molecular Dynamics
NAMD	Nanoscale Molecular Dynamics
PME	Particle mesh Ewald
MD	Molecular Dynamics
V_H	variable region of the antibody heavy chain
V_L	variable region of the antibody light chain
PCA	Principle Component Analysis
NMA	Normal Mode Analysis
DCCM	Dynamical Cross-Correlation Map
RMSF	root mean squared fluctuations
CDR	the antibody complementarity determining region
PC	principal component

Authorship statement

NIA, AAZ, RIL designed research; NIA and AAZ performed computer simulations; NIA, AAZ, RIL analyzed data; NIA, AAZ, TAN, RIL wrote the paper.

Supplementary material

The supplementary material for this paper is available online at http://dx.doi.org/10.1080/07391102.2015.1128979.

Disclosure statement

No potential conflict of interest was reported by the authors.

Funding

This work was supported by the Program for Competitive Growth of Kazan Federal University.

References

Akagawa, M., Ito, S., Toyoda, K., Ishii, Y., Tatsuda, E., Shibata, T., … Uchida, K. (2006). Bispecific Abs against modified protein and DNA with oxidized lipids. *Proceedings of the National Academy of Sciences, 103*, 6160–6165.

Akiba, H., & Tsumoto, K. (2015). Thermodynamics of antibody–antigen interaction revealed by mutation analysis of antibody variable regions. *Journal of Biochemistry, 158*, 1–13.

Ames, P. R. J., Alves, J., Murat, I., Isenberg, D. A., & Nourooz-Zadeh, J. (1999). Oxidative stress in systemic lupus erythematosus and allied conditions with vascular involvement. *Rheumatology, 38*, 529–534.

Avnir, Y., Tallarico, A. S., Zhu, Q., Bennett, A. S., Connelly, G., Sheehan, J., ... Marasco, W. A. (2014). Molecular signatures of hemagglutinin stem-directed heterosubtypic human neutralizing antibodies against influenza A viruses. *PLoS Pathogens, 10*, e1004103.

Bach, J. F., Koutouzov, S., & Endert, P. M. (1998). Are there unique autoantigens triggering autoimmune diseases? *Immunological Reviews, 164*, 139–155.

Behrendt, M., Partridge, L. J., Griffiths, B., & Goodfield, M. (2003). The role of somatic mutation in determining the affinity of anti-DNA antibodies. *Clinical and Experimental Immunology, 131*, 182–189.

Berendsen, H. J. C., Postma, J. P. M., van Gunsteren, W. F., DiNola, A., & Haak, J. R. (1984). Molecular dynamics with coupling to an external bath. *The Journal of Chemical Physics, 81*, 3684–3690.

Bespalov, I. A., Bond, J. P., Purmal, A. A., Wallace, S. S., & Melamede, R. J. (1999). Fabs specific for 8-oxoguanine: Control of DNA binding. *Journal of Molecular Biology, 293*, 1085–1095.

Casciola-Rosen, L., Wigley, F., & Rosen, A. (1997). Scleroderma autoantigens are uniquely fragmented by metal-catalyzed oxidation reactions: Implications for pathogenesis. *Journal of Experimental Medicine, 185*, 71–80.

Cerutti, M. L., Centeno, J. M., Goldbaum, F. A., & de Prat-Gay, G. (2001). Generation of sequence-specific, high affinity anti-dna antibodies. *Journal of Biological Chemistry, 276*, 12769–12773.

Collis, A. V., Brouwer, A. P., & Martin, A. C. (2003). Analysis of the antigen combining site: Correlations between length and sequence composition of the hypervariable loops and the nature of the antigen. *Journal of Molecular Biology, 325*, 337–354.

Demaison, C., Chastagner, P., Theze, J., & Zouali, M. (1994). Somatic diversification in the heavy chain variable region genes expressed by human autoantibodies bearing a lupus-associated nephritogenic anti-DNA idiotype. *Proceedings of the National Academy of Sciences, 91*, 514–518.

Dixit, K., & Ali, R. (2001). Antigen binding characteristics of antibodies induced against nitric oxide modified plasmid DNA. *Biochimica et Biophysica Acta (BBA) – General Subjects, 1528*, 1–8.

Dörner, T., Kaschner, S., Hansen, A., Pruss, A., & Lipsky, P. E. (2001). Perturbations in the impact of mutational activity on Vλ genes in systemic lupus erythematosus. *Arthritis Research, 3*, 368–374.

Edgar, R. C. (2004). MUSCLE: Multiple sequence alignment with high accuracy and high throughput. *Nucleic Acids Research, 32*, 1792–1797.

Evans, M. D., Cooke, M. S., Akil, M., Samanta, A., & Lunec, J. (2000). Aberrant processing of oxidative DNA damage in systemic lupus erythematosus. *Biochemical and Biophysical Research Communications, 273*, 894–898.

Foloppe, N., & MacKerell, A. D., Jr. (2000). All-atom empirical force field for nucleic acids: I. Parameter optimization based on small molecule and condensed phase macromolecular target data. *Journal of Computational Chemistry, 21*, 86–104.

Foster, M. H., Kieber-Emmons, T., Ohliger, M., & Madaio, M. P. (1994). Molecular and structural analysis of nuclear localizing anti-DNA lupus antibodies. *Immunologic Research, 13*, 186–206.

Fraser, N. L. W., Rowley, G., Field, M., & Stott, D. I. (2003). The V_H gene repertoire of splenic B cells and somatic hypermutation in systemic lupus erythematosus. *Arthritis Research & Therapy, 5*, R114–R121.

Frese, S., & Diamond, B. (2011). Structural modification of DNA – A therapeutic option in SLE? *Nature Reviews Rheumatology, 7*, 733–738.

Grant, B. J., Rodrigues, A., ElSawy, K., McCammon, J., & Caves, L. (2006). Bio3d: An R package for the comparative analysis of protein structures. *Bioinformatics, 22*, 2695–2696.

Greenspan, N. S., Lu, M. A., Shipley, J. W., Ding, X., Li, Q., Sultana, D., ... Emancipator, S. N. (2012). IgG3 deficiency extends lifespan and attenuates progression of glomerulonephritis in MRL/lpr mice. *Biology Direct, 7*, 3.

Hahn, B. H. (1998). Antibodies to DNA. *New England Journal of Medicine, 338*, 1359–1368.

Herron, J. N., He, X. M., Ballard, D. W., Blier, P. R., Pace, P. E., Bothwell, A. L. M., ... Edmundson, A. B. (1991). An autoantibody to single-stranded DNA: Comparison of the three-dimensional structures of the unliganded fab and a deoxynucleotide-fab complex. *Proteins: Structure, Function, and Genetics, 11*, 159–175.

Hideshi, Y., & Ryuta, M. (2014). Structural biology of DNA (6-4) photoproducts formed by ultraviolet radiation and interactions with their binding proteins. *International Journal of Molecular Sciences, 15*, 20321–20338.

Humphrey, W., Dalke, A., & Schulten, K. (1996). VMD: Visual molecular dynamics. *Journal of Molecular Graphics, 14*, 33–38.

Isenberg, D. A., Tucker, L. B., & Cambridge, G. (1997). Anti-MPO in adult- and childhood-onset SLE. *Rheumatology, 36*, 1343.

Jang, Y. J., & Stollar, B. D. (2003). Anti-DNA antibodies: Aspects of structure and pathogenicity. *Cellular and Molecular Life Sciences (CMLS), 60*, 309–320.

Kabat, E. A., Wu, T. T., Perry, H. M., Gottesman, K. S., & Foeller, C. (1991). *Sequences of proteins of immunological interest*. Bethesda, MD: National Institutes of Health.

Kobayashi, H., Morioka, H., Tobisawa, K., Torizawa, T., Kato, K., Shimada, I., … Ohtsuka, E. (1999). *Biochemistry, 38*, 532–539.

Kozyr, A. V., Kolesnikov, A. V., Khlyntseva, A. E. Bogun, A. G., Savchenko, G. A., Shemyakin, I. G., & Gabibov, A. G. (2012). Role of structure-based changes due to somatic mutation in highly homologous DNA-binding and DNA-hydrolyzing autoantibodies exemplified by A23P substitution in the VH domain. *Autoimmune Diseases, 2012*, Article ID 683829.

Krijnen, W. (2009). *Applied Statistics for Bioinformatics using R*. [Adobe Digital Editions version]. Retrieved from http://cran.cnr.berkeley.edu/doc/contrib/Krijnen-IntroBioInfStatistics.pdf

Krishnan, M. R., Wang, C., & Marion, T. N. (2012). Anti-DNA autoantibodies initiate experimental lupus nephritis by binding directly to the glomerular basement membrane in mice. *Kidney International, 82*, 184–192.

Kuroda, D., Shirai, H., Jacobson, M. P., & Nakamura, H. (2012). Computer-aided antibody design. *Protein Engineering, Design & Selection, 25*, 507–522.

Lunec, J., Herbert, K., Blount, S., Griffiths, H. R., & Emery, P. (1994). 8-Hydroxydeoxyguanosine. *FEBS Letters, 348*, 131–138.

MacKerell, A. D., Bashford, D., Bellott, M. L. D. R., Dunbrack, R. L., Evanseck, J. D., Field, M. J., & Fischer, S. (1998). All-atom empirical potential for molecular modeling and dynamics studies of proteins. *The Journal of Physical Chemistry B, 102*, 3586–3616.

Maeshima, E., Liang, X. M., Otani, H., Mune, M., & Yukawa, S. (2002). Effect of environmental changes on oxidative deoxyribonucleic acid (DNA) damage in systemic lupus erythematosus. *Archives of Environmental Health: An International Journal, 57*, 425–428.

McHugh, N. J. (2002). Systemic lupus erythematosus and dysregulated apoptosis – What is the evidence? *Rheumatology, 41*, 242–245.

Mol, C. D., Muir, A. K., Cygler, M., Lee, J. S., & Anderson, W. F. (1994). Structure of an immunoglobulin Fab fragment specific for triple-stranded DNA. *Journal of Biological Chemistry, 269*, 3615–3622.

Moolenaar, G. F., Hoglund, L., & Goosen, N. (2001). Clue to damage recognition by UvrB: Residues in the beta-hairpin structure prevent binding to non-damaged DNA. *The EMBO Journal, 20*, 6140–6149.

Morioka, H., Miura, H., Kobayashi, H., Koizumi, T., Fujii, K., Asano, K., ... Ohtsuka, E. (1998). Antibodies specific for (6-4) DNA photoproducts: Cloning, antibody modeling and construction of a single-chain Fv derivative. *Biochimica et Biophysica Acta (BBA) – Protein Structure and Molecular Enzymology, 1385*, 17–32.

Phillips, J. C., Braun, R., Wang, W., Gumbart, J., Tajkhorshid, E., Villa, E., … Schulten, K. (2005). Scalable molecular dynamics with NAMD. *Journal of Computational Chemistry, 26*, 1781–1802.

Pisetsky, D. S. (2013). Standardization of anti-DNA antibody assays. *Immunologic Research, 56*, 420–424.

Pokkuluri, P. R., Bouthillier, F., Li, Y., Kuderova, A., Lee, J., & Cygler, M. (1994). Preparation, characterization and crystallization of an antibody fab fragment that recognizes RNA. *Journal of Molecular Biology, 243*, 283–297.

Pyrkov, T. V., Chugunov, A. O., Krylov, N. A., Nolde, D. E., & Efremov, R. G. (2009). PLATINUM: A web tool for analysis of hydrophobic/hydrophilic organization of biomolecular complexes. *Bioinformatics, 25*, 1201–1202.

Radic, M. Z., & Seal, S. N. (1997). Selection of recurrent V genes and somatic mutations in autoantibodies to DNA. *Methods, 11*, 20–26.

Radic, M. Z., & Weigert, M. (1994). Genetic and structural evidence for antigen selection of Anti-DNA antibodies. *Annual Review of Immunology, 12*, 487–520.

Rahman, A., Giles, I., Haley, J., & Isenberg, D. (2002). Systematic analysis of sequences of anti-DNA antibodies – Relevance to theories of origin and pathogenicity. *Lupus, 11*, 807–823.

Ricci, V. (2005). *Fitting Distributions with R*. [Adobe Digital Editions version]. Retrieved from http://cran.r-project.org/doc/contrib/Ricci-distributions-en.pdf

Rosen, A., & Casciola-Rosen, L. (2009). Autoantigens in systemic autoimmunity: Critical partner in pathogenesis. *Journal of Internal Medicine, 265*, 625–631.

Saul, F. A., & Alzari, P. M. (1996). Crystallographic studies of antigen-antibody interactions. *Methods in Molecular Biology, 66*, 11–23.

Schuermann, J. P., Henzl, M. T., Deutscher, S. L., & Tanner, J. J. (2004). Structure of an anti-DNA fab complexed with a non-DNA ligand provides insights into cross-reactivity and molecular mimicry. *Proteins, 57*, 1097–0134.

Scrima, A., Koníčková, R., Czyzewski, B. K., Kawasaki, Y., Jeffrey, P. D., Groisman, R., ... Thomä, N. H. (2008). Structural basis of UV DNA-damage recognition by the DDB1–DDB2 complex. *Cell, 135*, 1213–1223.

Skorvaga, M., Theis, K., Mandavilli, B. S., Kisker, C., & Van Houten, B. (2002). The beta-hairpin motif of UvrB is essential for DNA binding, damage processing, and UvrC-mediated incisions. *Journal of Biological Chemistry, 277* (2), 1553–1559.

Stuart, L., & Hughes, J. (2002). Apoptosis and autoimmunity. *Nephrology, Dialysis, Transplantation, 17*, 697–700.

Su, K. Y., & Pisetsky, D. S. (2009). The role of extracellular DNA in autoimmunity in SLE. *Scandinavian Journal of Immunology, 70*, 175–183.

Sundberg, E. J. (2009). Structural basis of antibody–antigen interactions. *Methods in Molecular Biology, 524*, 23–36.

Suwannaroj, S., Lagoo, A., Keisler, D., & McMurray, R. W. (2001). Antioxidants suppress mortality in the female NZB × NZW F1 mouse model of systemic lupus erythematosus (SLE). *Lupus, 10*, 258–265.

Suzuki, N., Harada, T., Mihara, S., & Sakane, T. (1996). Characterization of a germline Vk gene encoding cationic anti-DNA antibody and role of receptor editing for development of the autoantibody in patients with systemic lupus erythematosus. *Journal of Clinical Investigation, 98*, 1843–1850.

Truglio, J. J., Karakas, E., Rhau, B., Wang, H., DellaVecchia, M. J., Van Houten, B., & Kisker, C. (2006). Structural basis for DNA recognition and processing by UvrB. *Nature Structural & Molecular Biology, 13*, 360–364.

Utz, P. J., Hottelet, M., Schur, P. H., & Anderson, P. (1997). Proteins phosphorylated during stress-induced apoptosis are common targets for autoantibody production in patients with systemic lupus erythematosus. *Journal of Experimental Medicine, 185*, 843–854.

Vargas-Madrazo, E., Lara-Ochoa, F., & Carlos Almagro, J. (1995). Canonical structure repertoire of the antigen-binding site of immunoglobulins suggests strong geometrical restrictions associated to the mechanism of immune recognition. *Journal of Molecular Biology, 254*, 497–504.

Waris, G., & Alam, K. (2004). Immunogenicity of superoxide radical modified-DNA: Studies on induced antibodies and SLE anti-DNA autoantibodies. *Life Sciences, 75*, 2633–2642.

Waszczykowska, E., Robak, E., Wozniacka, A., Narbutt, J., Torzecka, J. D., & Sysa-Jedrzejowska, A. (1999). Estimation of SLE activity based on the serum level of chosen cytokines and superoxide radical generation. *Mediators of Inflammation, 8*, 93–100.

Waters, S. T., McDuffie, M., Bagavant, H., Deshmukh, U. S., Gaskin, F., Jiang, C., … Fu, S. M. (2004). Breaking tolerance to double stranded DNA, nucleosome, and other nuclear antigens is not required for the pathogenesis of lupus glomerulonephritis. *Journal of Experimental Medicine, 199*, 255–264.

Yokoyama, H., Mizutani, R., & Satow, Y. (2013). Structure of a double-stranded DNA (6-4) photoproduct in complex with the 64M-5 antibody Fab. *Acta Cryst., D69*, 504–512.

Yokoyama, H., Mizutani, R., Satow, Y., Komatsu, Y., Ohtsuka, E., & Nikaido, O. (1999). Crystal structures of the 64M-2 and 64M-3 antibody Fabs complexed with DNA (6-4)photoproducts. *Nucleic Acids Symposium Series, 42*, 267–268.

Yokoyama, H., Mizutani, R., Satow, Y., Komatsu, Y., Ohtsuka, E., & Nikaido, O. (2000). Crystal structure of the 64M-2 antibody fab fragment in complex with a DNA dt(6–4)T photoproduct formed by ultraviolet radiation. *Journal of Molecular Biology, 299*, 711–723.

Yokoyama, H., & Mizutani, R. (2014). Structural biology of DNA (6-4) photoproducts formed by ultraviolet radiation and interactions with their binding proteins. *International Journal of Molecular Sciences, 15*, 20321–20338.

Yung, S., & Chan, T. M. (2008). Anti-DNA antibodies in the pathogenesis of lupus nephritis – The emerging mechanisms. *Autoimmunity Reviews, 7*, 317–321.

Zein, H. S., El-Sehemy, A. A., Fares, M. O., ElHefnawi, M., Teixeira da Silva, J. A., & Miyatake, K. (2011). Generation, characterization, and docking studies of DNA-hydrolyzing recombinant F_{ab} antibodies. *Journal of Molecular Recognition, 24*, 862–874.